Control of Photocurrent Generation in Polymer/ZnO Nanorod Solar Cells by Using a Solution-Processed TiO2 Overlayer

ARTICLE *in* JOURNAL OF PHYSICAL CHEMISTRY LETTERS · FEBRUARY 2010

Impact Factor: 7.46 · DOI: 10.1021/jz900356u

7 AUTHORS, INCLUDING:

Pedro Atienzar
Universitat Politècnica de València
60 PUBLICATIONS **2,025** CITATIONS
SEE PROFILE

Benoit Illy
Imperial College London
15 PUBLICATIONS **384** CITATIONS
SEE PROFILE

Jenny Nelson
Imperial College London
300 PUBLICATIONS **16,973** CITATIONS
SEE PROFILE

THE JOURNAL OF PHYSICAL CHEMISTRY Letters

pubs.acs.org/JPCL

Control of Photocurrent Generation in Polymer/ZnO Nanorod Solar Cells by Using a Solution-Processed TiO_2 Overlayer

Pedro Atienzar,*,† Thilini Ishwara,† Benoit N. Illy,§ Mary P. Ryan,§ Brian C. O'Regan,‡ James R. Durrant,‡ and Jenny Nelson†

†Department of Physics, ‡Department of Chemistry, and §Department of Materials, Imperial College London, London SW7 2AZ, United Kingdom

ABSTRACT We report herein the fabrication of hybrid conjugated polymer/ZnO photovoltaic devices using ZnO nanorod structures prepared by electrodeposition and study the effect of introducing a second metal oxide overlayer using a $TiCl_4$ post-treatment. We use transient absorption spectroscopy, scanning electron microscopy, and photovoltaic device measurements to study the microstructure and charge generation properties of the hybrid films and the performance of the resulting devices. We show how the ZnO nanostructure can be controlled via the nanorod growth conditions and demonstrate that photovoltaic device performance can be optimized by controlling the nanostructure in this way. Moreover, we show that a large increase in photocurrent generation can be achieved by coating the ZnO surface with a thin layer of titanium oxide by treating the ZnO nanostructure with a $TiCl_4$ solution.

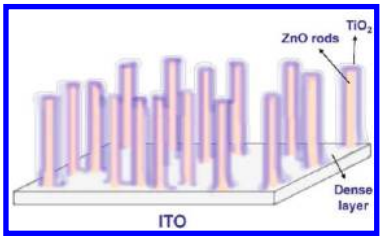

SECTION Electron Transport, Optical and Electronic Devices, Hard Matter

Photovoltaic devices based on molecular and nanostructured semiconductors are an alternative to conventional inorganic solar cells. The materials used in these types of devices present several advantages, such as easy processing, mechanical flexibility, and the potential low cost of large-area fabrication. They also offer potential applications in other optoelectronic devices such as light-emitting diodes and sensors.[1−3]

One of the more interesting advantages of hybrid solar cells based on conjugated polymers and metal oxides is the high electron mobility of the inorganic phase compared with that of available organic acceptor materials, particularly n-type polymers. An inorganic acceptor phase can be utilized to overcome the limited electron mobility in organic materials and so to help balance charge transport.[4,5] In addition, another important property of the inorganic materials is their higher physical and chemical stability relative to that of organic materials.

It is well-known that the morphology and the nanostructure of the different phases that form the devices have an important influence on the final properties.[5−9] For example, in the case of the inorganic phase, there are many examples of different kinds of metal oxide nanostructures that have been successfully integrated in devices, for instance, nanoparticles,[10] nanorods,[9,11] nanotubes,[12] or mesoporous networks,[13] giving in many cases an improved photovoltaic effect relative to that of simple layered structures.[5,11]

One of the most widely studied metal oxide semiconductors is zinc oxide, which is attractive for a variety of practical applications[14] due to its exceptional electrical, optical, and magnetic properties.[15] One important characteristic of ZnO is the huge family of structures that have been reported, such as nanowires, nanorods, tetrapods, and nanoribbons/belts among many others.[15] Moreover, there are several techniques that have been developed for the growth of ZnO nanostructures, including thermal evaporation, metal−organic vapor-phase epitaxy (MOVPE), metal−organic chemical vapor deposition (MOCVD), laser ablation, template-based synthesis, and electrodeposition. The electrodeposition technique is a low-temperature technique well-suited for cheap large-scale production. Additionally, electrodeposited ZnO nanorods have already shown great potential in nanostructured solar cells and electroluminescent hybrid light-emitting diodes.[16,17]

In order to maximize the performance of hybrid oxide/organic systems, it is necessary to control the oxide/polymer interface. Among the approaches used previously for this purpose are surface modification using amphiphilic molecular dyes[6] and the use of metal oxide coating layers.[18−20]

In this Letter, we first demonstrate the preparation of a nanostructured hybrid solar cell using zinc oxide nanorods prepared by electrodeposition. We then show how the modification of ZnO nanorods with a layer of TiO_2 leads to substantial increases in charge generation yield and hence to increased photocurrent generation in hybrid PV devices.

Received Date: December 3, 2009
Accepted Date: January 18, 2010
Published on Web Date: January 26, 2010

DOI: 10.1021/jz900356u | *J. Phys. Chem. Lett.* **2010**, *1*, 708–713

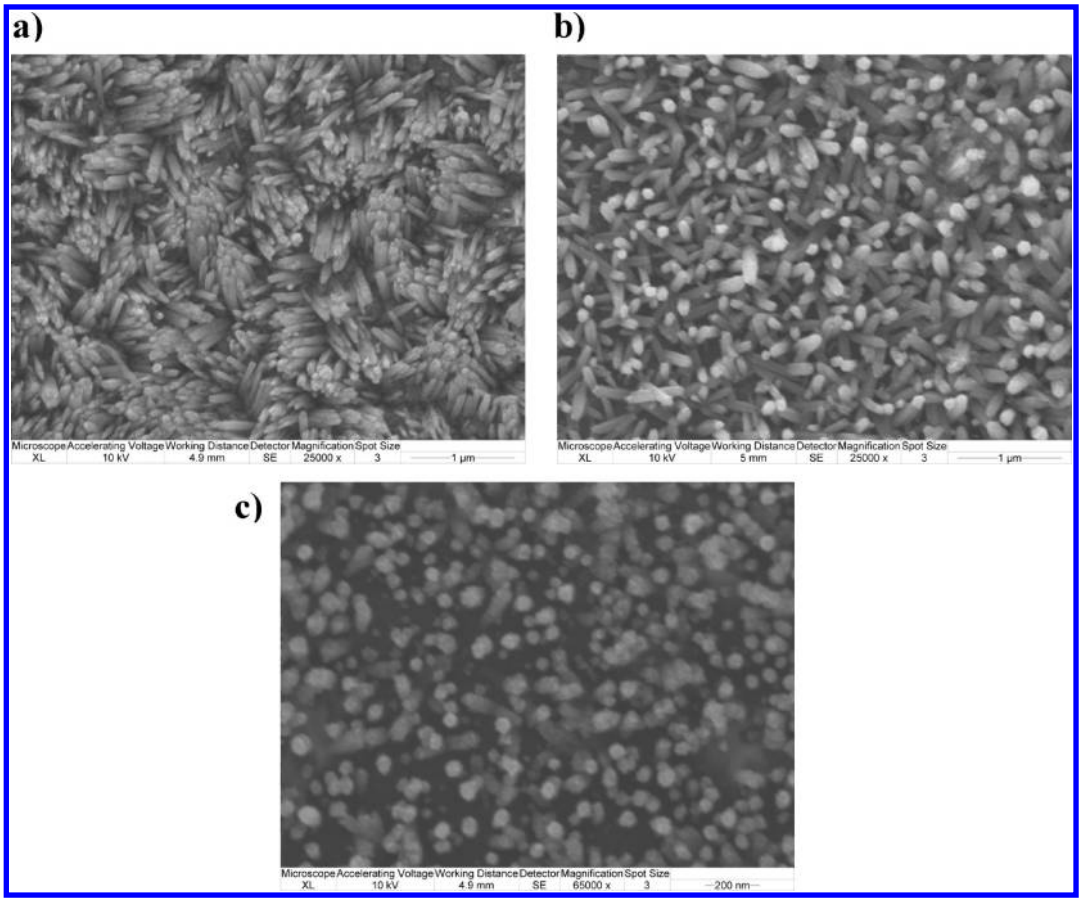

Figure 1. SEM images of ZnO nanorods at different $ZnCl_2$ concentrations, (a) 0.1, (b) 0.05, and (c) 0.01 mM.

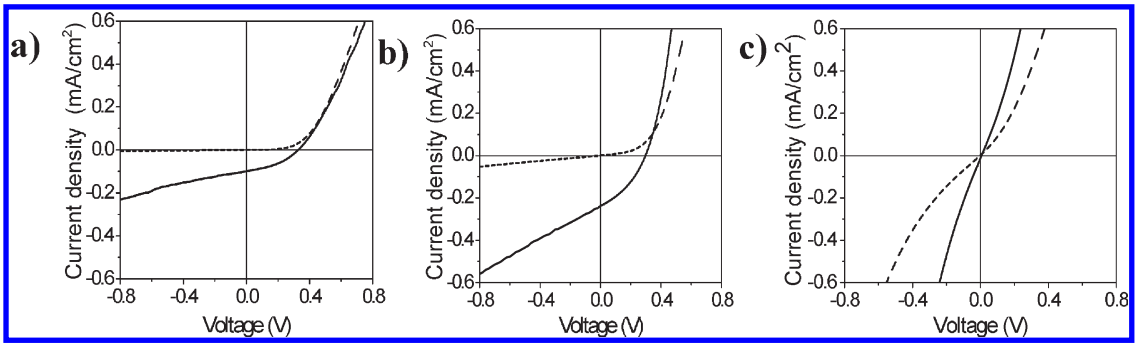

Figure 2. Characteristic $J-V$ curves of hybrid ITO/dense ZnO/ZnO rods/P3HT/PEDOT−PSS/Au devices made from ZnO rods prepared using different precursor concentrations, (a) 0.1, (b) 0.05, and (c) 0.01 mM. Solid and dashed lines correspond to illumination and dark current curves, respectively.

Scanning electron microscope (SEM) images of ZnO nanorods deposited at three different concentrations of the $ZnCl_2$ precursor (0.1, 0.05 and 0.01 mM) are shown in Figure 1. Analysis of the SEM images indicates that as the precursor concentration increases, the ZnO rod diameter increases slightly while the ZnO rod population increases markedly, as previously reported.[21,22] Very similar film thicknesses, between 200 and 300 nm, were obtained in all cases for similar deposition times.

In order to establish the optimum conditions for ZnO rod growth for use in hybrid solar cells, devices were prepared using regioregular poly(3-hexylthiophene) polymer (P3HT) as the donor material using the procedure described in the Experimental Section. Due to the conductive properties of the ZnO and the small thickness of the samples prepared, no extra coating was necessary to carry out the analysis by SEM, giving us the opportunity to prepare devices directly with the samples characterized by SEM. In Figure 2, the current density−voltage ($J-V$) curves of the devices are shown for several different $ZnCl_2$ precursor concentrations used during the electrodeposition process.

DOI: 10.1021/jz900356u | J. Phys. Chem. Lett. 2010, 1, 708–713

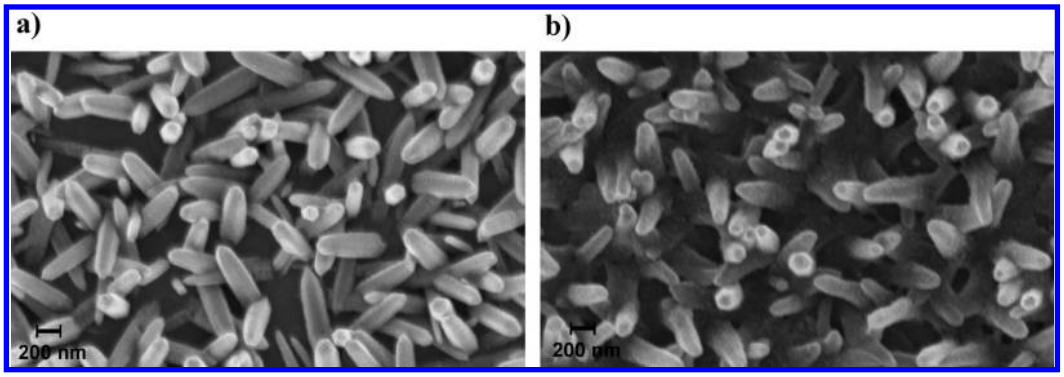

Figure 3. SEM images of ZnO nanorods (a) before and (b) after $TiCl_4$ treatment.

The highest photovoltaic power conversion efficiency is achieved at a precursor concentration of around 0.05 mM $ZnCl_2$. The better device performances in the case of the 0.05 mM concentration may be due to the optimum spacing of the nanorods. In the case of the 0.1 mM precursor concentration, the rod population appeared too high, and the rods were densely packed. This can cause difficulties in the polymer infiltration and therefore limit the polymer−metal oxide contact area. In the case where the concentration was 0.01 mM, the ZnO rod population was very low, and this reduced the available interface area for exciton dissociation by the nanostructures. It also left a larger area of the imperfectly blocking ZnO dense layer exposed, therefore enabling shunt losses. The above results correlate with charge generation studies using transient absorption spectroscopy, giving the highest signal when the concentration was 0.05 mM. Further studies are currently in progress in order to optimize other parameters in the electrodeposition process.

After establishing the optimum conditions in terms of ZnO precursor concentrations, we studied the effect of introducing a coating of a second metal oxide. The ZnO film was coated with a thin TiO_2 overlayer by dipping the ZnO nanorod film in a 50 mM aqueous solution of $TiCl_4$. The process is described in detail elsewhere.[20] In Figure 3, we show SEM images of the ZnO rods before and after the coating treatment. The images clearly show a layer that covers the surface of the ZnO rods. This was confirmed with elemental analysis using energy dispersive X-ray spectroscopy (EDAX) (see Supporting Information, Figure S1).

Several studies have been reported previously of the treatment of nanocrystalline TiO_2 electrodes with $TiCl_4$ solutions, resulting in a significant improvement in the performance of dye-sensitized solar cells. This treatment typically results in a significant improvement in J_{sc}.[19,20] We have observed a similar effect on the performance of the nanostructured hybrid solar cells prepared here. Figure 4 shows the comparative $J-V$ curves for devices made from ZnO rods that were and were not coated (also see Table 1). The current density increases from 0.24 to 0.53 mA/cm^2 upon introducing the coating. The open circuit voltage increases only slightly (0.30−0.32 V) upon coating, and the dark current decreases slightly, indicating that the effect of the coating is mainly on the net charge pair generation rather than on the electrical properties of the device. In addition, the fill factor increases

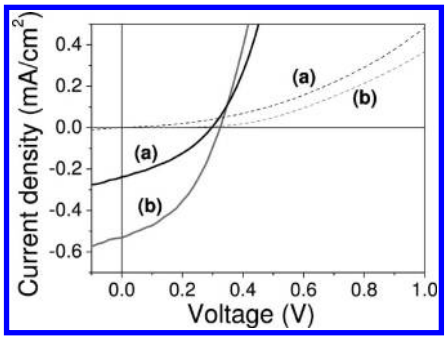

Figure 4. Comparative $J-V$ curve of ZnO rod samples (a) before $TiCl_4$ treatment and (b) after. The dashed lines correspond to the dark current curves.

Table 1. Performance of Hybrid Zinc Oxide Nanorod Solar Cells Prepared with and without TiO_2 Coating and Measured under Simulated AM 1.5 Solar Irradiation (100 mW/cm^2, 1 sun)

device	V_{oc} (V)	J_{sc} (mA/cm^2)	fill factor	efficiency (%)
before $TiCl_4$ treatment	0.30	0.24	0.36	0.025
after $TiCl_4$ treatment	0.32	0.53	0.41	0.070

from 0.36 to 0.41, and the overall power conversion efficiency increases by a factor of 2−3 relative to devices prepared without TiO_2 coating.

Transient Absorption Spectroscopy Measurements. In order to identify the origin of the increased photocurrent, transient absorption spectroscopy studies were carried out. By monitoring the photoinduced absorption of the polymer cation generated, we can estimate the relative yield of charge separation. We observe differences both in the yield of generated charge and in the dynamics of charge recombination. Figure 5 shows the effect of the $TiCl_4$ treatment on charge separation yield and decay kinetics.

The transient absorption spectra shows a broad band between 700 and 1000 nm that corresponds to the P3HT radical cation.[23] In both cases, a similar spectrum was observed (Figure 5a). However, important differences were observed in signal intensity and kinetics. First, the transient absorption signal was increased by approximately a factor of 3 by the $TiCl_4$ treatment. Second, the decay half-time increased from about 100 μs for the sample not coated with

DOI: 10.1021/jz900356u | J. Phys. Chem. Lett. 2010, 1, 708–713

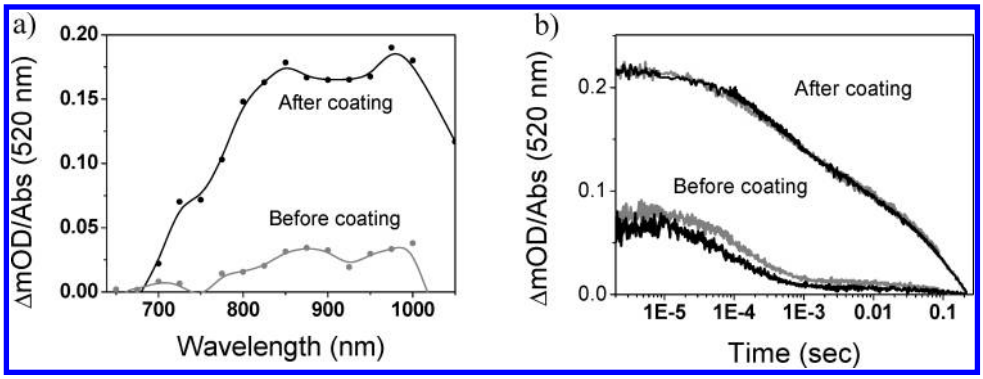

Figure 5. (a). Transient spectra recorded at 2 μs after 520 nm laser excitation of a sample before TiO_2 coating and after. (b) Comparative signal decay monitored at 950 nm before and after coating. The gray traces correspond to illumination through the ITO (front) and the black traces to illumination through the polymer (back).

TiO_2 to 8 ms after coating. Finally, we observe that after coating, the transient absorption signals for front- and back-side illumination are identical, indicating that the coating facilitates the infiltration of the polymer solution, resulting in good pore filling.[24]

This phenomenon of slowing the interfacial charge recombination between the injected electron and the hole from the polymer is analogous to that reported previously for dye-sensitized films,[19] where the retardation of recombination dynamics and the improvement in device performance with the $TiCl_4$-deposited TiO_2 layer was assigned to this layer acting as a physical barrier layer increasing the spatial separation of the electron and hole, therefore slowing the recombination dynamics.

In order to explain the observations herein, we consider the following factors. First, the $TiCl_4$-treated films shows a slightly increased porosity relative to the untreated film due to partial erosion of the nanorod structure. This is likely to improve polymer infiltration and therefore the contact area between the polymer and ZnO. This effect would result in increased TAS signal and hence in an increased photocurrent. However, it can not explain the slower recombination kinetics. The retardation in recombination kinetics can be attributed to the effect of the TiO_2 in achieving spatial separation between a hole in the polymer and an electron in the oxide, on account of the slightly higher conduction band edge of TiO_2 than ZnO. This tendency to spatial separation can be assigned to a slowing of bimolecular recombination. A final factor that should not be neglected is the possible effect of the higher dielectric permittivity of TiO_2 on reducing the binding energy of geminate charge pairs at the interface.

In conclusion, here, we show that the microstructure of hybrid polymer/ZnO films has an important influence on the performance characteristics of photovoltaic devices and that it can be controlled through the preparation conditions. Also, we demonstrate that coating with a second metal oxide is a valid method to control the interface of hybrid polymer−metal oxide solar cells. Transient absorption spectroscopy studies clearly indicate that the main effects of the metal oxide coating are to increase the charge generation yield and to slow the recombination rate. The main effect of the coating is to increase the photocurrent produced by photovoltaic devices, in agreement with the increased charge generation observed by transient spectroscopy.

EXPERIMENTAL SECTION

Electrodeposition of ZnO Rods. The electrodeposition of ZnO nanorods was performed in a standard three-electrode electrochemical cell with an indium tin oxide (ITO)-coated glass substrate as the working electrode, a Pt wire as the counter electrode, and a standard calomel electrode (SCE) as the reference electrode.[25] The electrolyte consisted of an aqueous solution of $ZnCl_2$ as the ZnO precursor, where the concentration was varied between 0.1 and 0.01 mM, containing 0.1 M KCl as the supporting electrolyte and saturated with oxygen. The ZnO nanorods were electrodeposited at 80 °C under a constant potential of −1.0 V versus SCE for 45 min.

All of the samples were prepared on ITO-coated glass substrates of area ∼1 cm^2 from Psiotec Ltd. which were first cleaned by ultrasonic agitation in acetone and isopropanol. The cleaned substrate was then coated with a dense ZnO layer, about 50 nm thick, using spray pyrolysis.[11] This layer functions both as a hole-blocking layer to prevent charge leakage by hole transfer between the polymer and ITO and as a seed layer for the subsequent growth of nanorods.[26]

$TiCl_4$ Treatment. The TiO_2 overlayer was applied by soaking the ZnO nanorod samples in a 50 mM $TiCl_4$ solution for 1 min at 70 °C, followed by a water rinse and heating at 400 °C for 20 min.[18,20] After several assays, the optimum dipping time proved to be only 1 min, in contrast to dye-sensitized solar cells (DSSCs) based on mesoporous TiO_2, where about 30 min is needed for complete coverage.[18] This difference can be explained in terms of the thickness of the ZnO nanorod film (which is a few hundreds of nanometres for our samples, while in DSSCs, the thickness is more than 5 μm) and the large dimensions of the ZnO rods compared to TiO_2 colloids. Both factors result in a much smaller surface area relative to the geometric area for the ZnO rods than that for a porous TiO_2 electrode. Therefore, it appears that this shorter dipping time is sufficient to coat the total surface of the ZnO rod film.

Preparation of Photovoltaic Devices. The electrodeposited ZnO rods were infiltrated with the polymer by immersing in a solution (∼2 mg/mL) of poly(3-hexylthiophene) (P3HT) in chlorobenzene at 110 °C overnight. Then, a thin layer,

DOI: 10.1021/jz900356u | J. Phys. Chem. Lett. 2010, 1, 708–713

~100 nm of P3HT, was deposited on the top of all of the samples by spin coating and annealing for 2 h at 140 °C in a nitrogen-filled glovebox. Sample preparation was completed by spin coating a layer (50 nm) of poly(3,4-ethylenedioxythiophene)−poly(styrenesulfonate, PEDOT−PSS (BAYTRON P, HC Stark, standard grade) on top of the P3HTand drying at 110 °C for 10 min on a hot plate before depositing gold by thermal evaporation. The thickness of all of the films was measured by a Tencor Alpha-Step 200 profilometer.

Transient absorption studies were carried out as described previously.[27] Devices were characterized by measuring the current density−voltage (*J*-V) characteristic in vacuum under simulated AM1.5 solar illumination (100 mW/cm^2).[28]

SUPPORTING INFORMATION AVAILABLE

Supporting figures and energy level diagram. This material is available free of charge via the Internet at http://pubs.acs.org.

AUTHOR INFORMATION

Corresponding Author:

*To whom correspondence should be addressed. E-mail: p.atienzar@imperial.ac.uk.

ACKNOWLEDGMENT P.A. acknowledges the Spanish Ministry of Science and Innovation for its financial support in the Postdoctoral grant, T.I. acknowledges the Dorothy Hodgkin postgraduate awards, and J.N. acknowledges support of the EPSRC through Research Grant GR/T26559 and the Excitonic Solar Cell Supergen Programme (Excitonic Supergen Consortium) and EP/E036341 (High-efficiency Hybrid Solar Cells for Microgeneration).

REFERENCES

(1) Keivanidis, P. E.; Greenham, N. C.; Sirringhaus, H.; Friend, R. H.; Blakesley, J. C.; Speller, R.; Campoy-Quiles, M.; Agostinelli, T.; Bradley, D. D. C.; Nelson, J. X-ray Stability and Response of Polymeric Photodiodes for Imaging Applications. *Appl. Phys. Lett.* **2008,** 92.

(2) Hoppe, H.; Sariciftci, N. S. Organic Solar Cells: An Overview. *J. Mater. Res.* **2004,** *19*, 1924–1945.

(3) Burroughes, J. H.; Bradley, D. D. C.; Brown, A. R.; Marks, R. N.; Mackay, K.; Friend, R. H.; Burns, P. L.; Holmes, A. B. Light-Emitting-Diodes Based on Conjugated Polymers. *Nature* **1990,** *347*, 539–541.

(4) Beek, W. J. E.; Wienk, M. M.; Janssen, R. A. J. Hybrid Polymer Solar Cells Based on Zinc Oxide. *J. Mater. Chem.* **2005,** *15*, 2985–2988.

(5) Huynh, W. U.; Dittmer, J. J.; Alivisatos, A. P. Hybrid Nanorod−Polymer Solar Cells. *Science* **2002,** *295*, 2425–2427.

(6) Ravirajan, P.; Peiro, A. M.; Nazeeruddin, M. K.; Graetzel, M.; Bradley, D. D. C.; Durrant, J. R.; Nelson, J. Hybrid Polymer/Zinc Oxide Photovoltaic Devices with Vertically Oriented ZnO Nanorods and an Amphiphilic Molecular Interface Layer. *J. Phys. Chem. B* **2006,** *110*, 7635–7639.

(7) Boucle, J.; Ravirajan, P.; Nelson, J. Hybrid Polymer−Metal Oxide Thin Films for Photovoltaic Applications. *J. Mater. Chem.* **2007,** *17*, 3141–3153.

(8) Schwartz, B. J. Conjugated Polymers As Molecular Materials: How Chain Conformation and Film Morphology Influence Energy Transfer and Interchain Interactions. *Annu. Rev. Phys. Chem.* **2003,** *54*, 141–172.

(9) Olson, D. C.; Piris, J.; Collins, R. T.; Shaheen, S. E.; Ginley, D. S. Hybrid Photovoltaic Devices of Polymer and ZnO Nanofiber Composites. *Thin Solid Films* **2006,** *496*, 26–29.

(10) Oregan, B.; Gratzel, M. A Low-Cost, High-Efficiency Solar-Cell Based on Dye-Sensitized Colloidal TiO_2 Films. *Nature* **1991,** *353*, 737–740.

(11) Peiro, A. M.; Ravirajan, P.; Govender, K.; Boyle, D. S.; O'Brien, P.; Bradley, D. D. C.; Nelson, J.; Durrant, J. R. Hybrid Polymer/Metal Oxide Solar Cells Based on ZnO Columnar Structures. *J. Mater. Chem.* **2006,** *16*, 2088–2096.

(12) Paulose, M.; Shankar, K.; Varghese, O. K.; Mor, G. K.; Hardin, B.; Grimes, C. A. Backside Illuminated Dye-Sensitized Solar Cells Based on Titania Nanotube Array Electrodes. *Nanotechnology* **2006,** *17*, 1446–1448.

(13) Atienzar, P.; Navarro, M.; Corma, A.; Garcia, H. Photovoltaic Activity of Ti/MCM-41. *ChemPhysChem* **2009,** *10*, 252–256.

(14) Ozgur, U.; Alivov, Y. I.; Liu, C.; Teke, A.; Reshchikov, M. A.; Dogan, S.; Avrutin, V.; Cho, S. J.; Morkoc, H. A Comprehensive Review of ZnO Materials and Devices. *J. Appl. Phys.* **2005,** 98.

(15) Aleksandra, B. D.; cacute; Leung, Y. H. Optical Properties of ZnO Nanostructures. *Small* **2006,** *2*, 944–961.

(16) Konenkamp, R.; Word, R. C.; Godinez, M. Ultraviolet Electroluminescence from ZnO/Polymer Heterojunction Light-Emitting Diodes. *Nano Lett.* **2005,** *5*, 2005–2008.

(17) Chen, Z. G.; Tang, Y. W.; Zhang, L. S.; Luo, L. J. Electrodeposited Nanoporous ZnO Films Exhibiting Enhanced Performance in Dye-Sensitized Solar Cells. *Electrochim. Acta* **2006,** *51*, 5870–5875.

(18) Sommeling, P. M.; O'Regan, B. C.; Haswell, R. R.; Smit, H. J. P.; Bakker, N. J.; Smits, J. J. T.; Kroon, J. M.; van Roosmalen, J. A. M. Influence of a $TiCl_4$ Post-treatment on Nanocrystalline TiO_2 Films in Dye-Sensitized Solar Cells. *J. Phys. Chem. B* **2006,** *110*, 19191–19197.

(19) Palomares, E.; Clifford, J. N.; Haque, S. A.; Lutz, T.; Durrant, J. R. Control of Charge Recombination Dynamics in Dye Sensitized Solar Cells by the Use of Conformally Deposited Metal Oxide Blocking Layers. *J. Am. Chem. Soc.* **2003,** *125*, 475–482.

(20) O'Regan, B. C.; Durrant, J. R.; Sommeling, P. M.; Bakker, N. J. Influence of the $TiCl_4$ Treatment on Nanocrystalline TiO_2 Films in Dye-Sensitized Solar Cells. 2. Charge Density, Band Edge Shifts, And Quantification of Recombination Losses at Short Circuit. *J. Phys. Chem. C* **2007,** *111*, 14001–14010.

(21) Elias, J.; Tena-Zaera, R.; Lévy-Clément, C. Electrochemical Deposition of ZnO Nanowire Arrays with Tailored Dimensions. *J. Electroanal. Chem.* **2008,** *621*, 171–177.

(22) Belghiti, H. E.; Pauporté, T.; Lincot, D. Mechanistic Study of ZnO Nanorod Array Electrodeposition. *Phys. Status Solidi A* **2008,** *205*, 2360–2364.

(23) Boucle, J.; Chyla, S.; Shaffer, M. S. P.; Durrant, J. R.; Bradley, D. D. C.; Nelson, J. Hybrid Solar Cells from a Blend of Poly(3-hexylthiophene) and Ligand-Capped TiO_2 Nanorods. *Adv. Funct. Mater.* **2008,** *18*, 622–633.

(24) Ravirajan, P. H.; S., A.; Durrant, J. R.; Poplavskyy, D.; Bradley, D. D. C.; Nelson, J. Hybrid Nanocrystalline TiO_2 Solar Cells with a Fluorene−Thiophene Copolymer As a Sensitizer and Hole Conductor. *J. Appl. Phys.* **2004,** *95*, 1473–1480.

(25) Tena-Zaera, R.; Elias, J.; Lévy-Clément, C.; Bekeny, C.; Voss, T.; Mora-Seró, I.; Bisquert, J. Influence of the Potassium Chloride Concentration on the Physical Properties of Electrodeposited ZnO Nanowire Arrays. *J. Phys. Chem. C* **2008,** *112*, 16318–16323.

(26) Elias, J.; Tena-Zaera, R.; Lévy-Clément, C. Electrodeposition of ZnO Nanowires with Controlled Dimensions for

Photovoltaic Applications: Role of Buffer Layer. *Thin Solid Films* **2007,** *515*, 8553–8557.

(27) Tachibana, Y.; Moser, J. E.; Gratzel, M.; Klug, D. R.; Durrant, J. R. Subpicosecond Interfacial Charge Separation in Dye-Sensitized Nanocrystalline Titanium Dioxide Films. *J. Phys. Chem.* **1996,** *100*, 20056–20062.

(28) Ishwara, T.; Bradley, D. D. C.; Nelson, J.; Ravirajan, P.; Vanseveren, I.; Cleij, T.; Vanderzande, D.; Lutsen, L.; Tierney, S.; Heeney, M.; McCulloch, I. Influence of Polymer Ionization Potential on the Open-Circuit Voltage of Hybrid Polymer/TiO_2 Solar Cells. *Appl. Phys. Lett.* **2008,** 92.

DOI: 10.1021/jz900356u | *J. Phys. Chem. Lett.* **2010,** *1*, 708–713